Journal of Molecular Structure 1198 (2019) 126874

Contents lists available at ScienceDirect

Journal of Molecular Structure

journal homepage: http://www.elsevier.com/locate/molstruc

Cyclic amines homobimetallic ruthenium pre-catalysts bearing bidentate phosphine and their dual catalytic activity for the ring-opening metathesis and atom-radical polymerizations

Patrik D.S. Gois [a], Thais R. Cruz [a], Daniele M. Martins [b], Antonio E.H. Machado [c, 1], André L. Bogado [d], Benedito S. Lima-Neto [b], Beatriz E. Goi [a], Valdemiro P. Carvalho Jr. [a, *]

[a] Faculdade de Ciências e Tecnologia, UNESP Univ Estadual Paulista, CEP 19060-900, Presidente Prudente, SP, Brazil
[b] Instituto de Química de São Carlos, Universidade de São Paulo, CEP 13560-970, São Carlos, SP, Brazil
[c] Instituto de Química, Universidade Federal de Uberlândia, P.O. Box 593, Uberlândia, 38400-089, Minas Gerais, Brazil
[d] Instituto de Ciências Exatas e Naturais Do Pontal, Universidade Federal de Uberlândia, Rua Vinte, 1600, CEP 38304-402, Ituiutaba, MG, Brazil

ARTICLE INFO

Article history:
Received 17 June 2019
Received in revised form
30 July 2019
Accepted 31 July 2019
Available online 1 August 2019

Keywords:
ROMP
ATRP
Norbornene
Methyl methacrylate
Homogenous catalysis

ABSTRACT

A series of [RuCl(dppb)(μ-Cl)$_3$Ru(dppb)(amine)] complexes, where amine is pyrrolidine (**1**), piperidine (**2**) or perhydroazepine (**3**), were synthesized and characterized by elemental analysis, FTIR, UV–Vis, and ^{1}H, ^{13}C{^{1}H} and ^{31}P{^{1}H} NMR spectroscopy. The electrochemistry properties of the complexes **1**–**3** were investigated by cyclic voltammetry and exhibited two successive single-electron oxidation processes. The presence of two redox pairs suggests the formation of a dimeric species in which two different fragments, {Ru(amine)(dppb)} and {RuCl(dppb)}, were connected via three μ-chloro bridges. The complexes **1**–**3** were evaluated as catalytic precursors for ROMP of norbornene (NBE) and norbornadiene (NBD), as well as for ATRP of methyl methacrylate (MMA). The polynorbornene (polyNBE) syntheses via ROMP using the complexes **1**–**3** as pre-catalysts were assessed under reaction conditions of [EDA]/[Ru] = 28 (5 μL) and [NBE]/[Ru] = 5000 as a function of time at 25 or 50 °C. Polymerization of MMA via ATRP was conducted using the complexes **1**–**3** in the presence of ethyl 2-bromoisobutyrate (EB*i*B) as initiator. Differences in the catalytic activities and polymerization controls were observed in the order **3** > **2** > **1** for both reactions. The activities were discussed considering the steric hindrance and electronic characteristics of the amines as ancillary ligands in the metal center using cyclic voltammetry and NMR studies.

1. Introduction

Currently, the combination of different multiple types of living polymerization methods has been the subject of intense study. Atom-transfer radical (ATRP) and ring-opening metathesis (ROMP) polymerizations are two of the most widely used polymerization methods in synthetic polymer chemistry that can be combined to synthetize new polymeric materials with controlled design and architecture [1–8].

ATRP is based on a dynamic equilibrium between active propagating radicals and dormant species. This equilibrium is established through reversible transition metal-catalyzed homolytic cleavage of a covalent carbon-halogen bond in the dormant species [9–14]. ROMP of cyclic olefins is a powerful transition metal-catalyzed reaction for synthesis of (co)polymers. It is a type of olefin metathesis reaction that reacts by opening the ring upon cross-linking of the olefinic carbons, resulting in a polymer with unsaturation retention in the backbone [15–19].

Synthesis of new catalysts has been directed towards optimizing two catalytic systems [20–24]. Some requirements are necessary to synthetize an efficient dual catalyst: first, it is necessary to choose the correct metal center because the metal weight, oxidation state, electronic density and selectivity for certain organic groups define the type of reaction in which the metal can be used; second, the correct choice of the ligands is also very important because the type of bond between metal center and ligand directs the specificity of use for the complex.

Our research group has been studying ROMP and ATRP from novel non-carbene Ru-based complexes [25–33]. Many of these

* Corresponding author.
E-mail addresses: valdemiro.carvalho@unesp.br, valdemiropcj@gmail.com (V.P. Carvalho).
[1] During his stay as Visiting Professor at the Programa de Pós-Graduação em Ciência e Tecnologia, at Universidade Federal de Goiás. Catalão, Goiás, Brazil.

https://doi.org/10.1016/j.molstruc.2019.126874
0022-2860/

compounds have exhibited good activity, forming polymers and copolymers in high yields, with different thermal and morphological characteristics. For example, complexes of the [$RuCl_2(PPh_3)_2$(-amine)] type quantitatively have produced polymers from norbornene (NBE) and norbornadiene (NBD) at room temperature and controlled the methyl methacrylate and styrene polymerization via ATRP. The electronic combination of a π-acceptor phosphine with a σ-donor amine has been a convenient modular approach to tune the reactivity of such initiators when varying their moieties, in addition to presenting appropriate steric hindrance.

This study evaluated the application of [RuCl(dppb)(μ-$Cl)_3$Ru(dppb)(amine)] complexes (Fig. 1), where amine = pyrrolidine (**1**), piperidine (**2**), or perhydroazepine (**3**), as versatile catalyst precursors for ROMP of norbornene (NBE) and norbornadiene (NBD), as well as for ATRP of methyl methacrylate (MMA) under different conditions of temperature and reaction time. The purpose was to observe the influence of a bidentate diphosphine ligand (dppb) on the reactivity of ruthenium catalysts bearing different cyclic amines, interpreting the subtle changes in the electronic and steric parameters of the catalytic systems to obtain resources to understand the features that influence ROMP and ATRP efficiency. In addition to amines, the dppb ligand can also drive the catalytic activity by controlling the electronic density or steric effect in the coordination metal sphere. Despite its importance, this ligand has not been widely explored in ROMP and ATRP.

2. Experimental

2.1. General remarks

Unless otherwise stated, all syntheses and manipulations were performed under nitrogen atmosphere following standard Schlenk techniques. Solvents were distilled from appropriate drying agents and deoxygenated prior to use. Methyl methacrylate (MMA) was washed with 5% NaOH solution, dried over anhydrous $MgSO_4$, vacuum distilled from CaH_2 and stored under nitrogen at −18 °C before use. 2,2,6,6-tetramethyl-1-piperidinoxyl (TEMPO), ferrocene (Fc), norbornene (NBE), norbornadiene (NBD), ethyl diazoacetate (EDA), pyrrolidine (pop), piperidine (pip), perhydroazepine (pep), triphenylphosphine (PPh_3), 1,4-bis(diphenylphosphino)butane (dppb), and ethyl 2-bromoisobutyrate (EB*i*B) were obtained from Aldrich and used as acquired. The [$RuCl_2$(dppb)(PPh_3)] complex was prepared following the literature and its purity was checked by satisfactory elemental analysis and spectroscopic examination (NMR, FTIR, and EPR) [25].

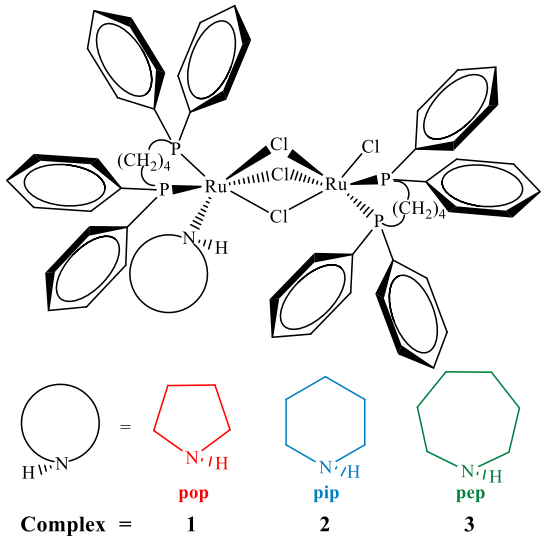

Fig. 1. Illustration of the amine homobimetallic ruthenium catalysts **1**–**3**.

2.2. Analyses

Elemental analyses were performed with a PerkinElmer CHN 2400 at the Elemental Analysis Laboratory of Institute of Chemistry - USP. The FTIR spectra were obtained on a Bomem FTIR MB 102. Electronic spectra were recorded on a Shimadzu (model UV-1800) spectrophotometer, using 1 cm path length quartz cells. The ^1H, $^{13}C\{^1H\}$ and $^{31}P\{^1H\}$ NMR spectra were obtained in $CDCl_3$ at 298 K on a Bruker DRX-400 spectrometer operating at 400.13, 100.62 and 161.98 MHz, respectively. Chemical shifts are listed in parts per million downfield from TMS and are referenced from the solvent peaks or TMS. Conversion was determined from the concentration of residual monomer measured by gas chromatography (GC) using a Shimadzu GC-2010 gas chromatograph equipped with a flame ionization detector and a 30 m (0.53 mm I.D., 0.5 μm film thickness) SPB-1 Supelco fused silica capillary column. Anisole was added to polymerization and used as an internal standard. Analysis conditions: injector and detector temperature, 250 °C; temperature program, 40 °C (4 min), 20 °C min^{-1} until 200 °C, 200 °C (2 min). The molecular weights and the molecular weight distribution of the polymers were determined by gel permeation chromatography using a Shimadzu Prominence LC system equipped with a LC-20AD pump, a DGU-20A5 degasser, a CBM-20A communication module, a CTO-20A oven at 40 °C and a RID-10A detector equipped with two Shimadzu columns (GPC-805: 30 cm, Ø = 8.0 mm). The retention time was calibrated with poly(methyl methacrylate) standards using HPLC-grade THF as an eluent at 40 °C with a flow rate of 1.0 mL min^{-1}. Electrochemical measurements were performed using an Autolab PGSTAT204 potentiostat with a stationary platinum disk and a wire as working and auxiliary electrodes, respectively. The reference electrode was Ag/AgCl. The measurements were performed at 25 °C ± 0.1 in CH_2Cl_2 with 0.1 mol L^{-1} of *n*-Bu_4NPF_6.

2.3. Syntheses of [RuCl(dppb)(μ-Cl)$_3$Ru(dppb)(amine)] (**1**–**3**)

The amine (pyrrolidine, piperidine, or perhydroazepine; 0.42 mmol) was added to a solution of [$RuCl_2(PPh_3)$(dppb)] (0.26 mmol; 0.22 g) in acetone (40 mL) and the resulting dark green solution was stirred for 12 h at room temperature. A yellow precipitate was then filtered and washed with acetone and ethyl ether and then dried under vacuum.

Complex **1**: Yield: 74%; Analytical data for $C_{60}H_{65}Cl_4NP_4Ru_2$ was 56.38C, 5.32 H and 1.08% N; Calcd. 56.83C, 5.17H and 1.10% N. UV–vis: $\lambda_{max(n)}$ (nm), $\varepsilon_{max(n)}$ [$M^{-1}cm^{-1}$]: $\lambda_{max(1)}$ (230), $\varepsilon_{max(1)}$ [50500]; $\lambda_{max(2)}$ (243), $\varepsilon_{max(2)}$ [35700]; $\lambda_{max(3)}$ (290), $\varepsilon_{max(3)}$ [5500]; $\lambda_{max(4)}$ (380), $\varepsilon_{max(4)}$ [2000]; $\lambda_{max(5)}$ (486), $\varepsilon_{max(5)}$ [320]; FTIR in CsI: 309 and 267 cm^{-1} [w; ν(Ru–Cl)] was found; 3245 cm^{-1} [w; ν(pop N–H)]. ^1H NMR ($CDCl_3$, 400 MHz) ppm: 8.35–6.82 (m, 40H, CH Ar), 3.7 (s, 1H, NH), 3.1–0.45 (m, 24H, CH_2) ppm; $^{13}C\{^1H\}$ NMR ($CDCl_3$, 100.6 MHz) ppm: 140.3, 140.1, 139.9, 137.0, 136.8, 136.7, 134.0, 133.2, 128.5, 127.6, 126.8, 126.0, 30.9, 29.4, 29.3, 29.1, 22.9 ppm; $^{31}P\{^1H\}$ NMR ($CDCl_3$, 162 MHz) ppm: 49.0 (s).

Complex **2**: Yield: 75%; Analytical data for $C_{61}H_{67}Cl_4NP_4Ru_2$ was 57.31C, 5.38 H and 1.02% N; Calcd. 57.15C, 5.27H and 1.09% N. UV–vis: $\lambda_{max(n)}$ (nm), $\varepsilon_{max(n)}$ [$M^{-1}cm^{-1}$]: $\lambda_{max(1)}$ (230), $\varepsilon_{max(1)}$ [50500]; $\lambda_{max(2)}$ (243), $\varepsilon_{max(2)}$ [35200]; $\lambda_{max(3)}$ (290), $\varepsilon_{max(3)}$ [5500]; $\lambda_{max(4)}$ (380), $\varepsilon_{max(4)}$ [2000]; $\lambda_{max(5)}$ (486), $\varepsilon_{max(5)}$ [300]; FTIR in CsI: 310 and 260 cm^{-1} [w; ν(Ru–Cl)] was found; 3251 cm^{-1} [w; ν(pip N–H)]. ^1H NMR (400 MHz, $CDCl_3$): δ = 8.36–6.79 (m, 40H, CH Ar), 3.7 (s, 1H, NH), 3.1–0.45 (m, 26H, CH_2) ppm; $^{13}C\{^1H\}$ NMR ($CDCl_3$): δ = 140.4, 140.2, 140.0, 136.9, 136.7, 136.6, 134.0, 133.2, 128.5, 127.6,

126.8, 126.0, 30.9, 29.4, 29.3, 29.1, 22.6 ppm; $^{31}P\{^{1}H\}$ NMR ($CDCl_3$: δ, ppm): 49.0 (s).

Complex **3**: Yield: 70%; Analytical data for $C_{62}H_{69}Cl_4NP_4Ru_2$ was 56.32C, 5.38 H and 1.02% N; Calcd. 57.46C, 5.37H and 1.08% N. UV–vis: $\lambda_{max(n)}$ (nm), $\varepsilon_{max(n)}$ [$M^{-1}cm^{-1}$]: $\lambda_{max(1)}$ (230), $\varepsilon_{max(1)}$ [39700]; $\lambda_{max(2)}$ (243), $\varepsilon_{max(2)}$ [26700]; $\lambda_{max(3)}$ (290), $\varepsilon_{max(3)}$ [3500]; $\lambda_{max(4)}$ (380), $\varepsilon_{max(4)}$ [1750]; $\lambda_{max(5)}$ (486), $\varepsilon_{max(5)}$ [50]; FTIR in CsI: 309 and 263 cm^{-1} [w; ν(Ru–Cl)] was found; 3253 cm^{-1} [w; ν(pep N–H)].^{1}H NMR (400 MHz, $CDCl_3$): $\delta = 7.55–6.96$ (m, 40H, CH Ar), 3.4 (s, 1H, NH), 3.1–0.45 (m, 28H, CH_2) ppm; $^{13}C\{^{1}H\}$ NMR ($CDCl_3$): $\delta = 140.4, 140.2, 140.0, 136.9, 136.7, 136.6, 134.0, 133.2, 128.5, 127.6, 126.8, 126.0, 26.6, 24.9, 22.8$ ppm; $^{31}P\{^{1}H\}$ NMR ($CDCl_3$: δ, ppm): 49.0 (s).

2.4. ROMP procedure

In a typical ROMP experiment, 1.1 μmol of complex was dissolved in $CHCl_3$ (2 mL) with an appropriate amount of monomer (NBE, NBD or DCPD; 5.5 mmol), followed by addition of carbene source (EDA; 31 μmol). The reaction mixture was stirred up to 60 min at 25 and 50 °C in a silicon oil bath. At room temperature, 5 mL of methanol was added and the polymer was filtered, washed with methanol and dried in a vacuum oven at 40 °C up to constant weight. The reported yields are average values from catalytic runs performed at least three times. The isolated polyNBEs were dissolved in THF for GPC data.

2.5. ATRP procedure

In a typical ATRP experiment, 12 μmol of complex was placed in a Schlenk tube containing a magnet bar and capped by a rubber septum. Air was expelled by three vacuum-nitrogen cycles and monomer (MMA; 12 mmol) and the initiator solution (EB*i*B, 24 μmol) were added. All liquids were handled with dried syringes under nitrogen. The tube was capped under N_2 atmosphere using Schlenk techniques, then the reaction mixture was immediately immersed in an oil bath previously heated to the desired temperature. The samples were removed from the tube after certain time intervals using degassed syringes. The polymerization was stopped when the reaction mixture became very viscous. The reported conversions are average values from catalytic runs performed at least three times.

3. Results and discussion

3.1. Synthesis and characterization of [RuCl(dppb)(μ-Cl)$_3$Ru(dppb)(amine)] (*1*–*3*)

Complexes **1**–**3** were synthesized from the reaction of complex [$RuCl_2(PPh_3)$(dppb)] with a 2-fold excess of amine (pop, pip, or pep) NMR time scalein acetone at room temperature (Scheme 1). After 12 h of reaction, the complexes **1**–**3** were obtained as a fine yellow powder precipitate, and a simple workup involving solvent filtration and the washing of the excess amine with diethyl ether resulted in the new binuclear amine-ruthenium-dppb complexes **1**–**3**. Our procedure closely matched the one reported by Fogg et al. for the preparation of dinuclear ruthenium-dppb compounds [34,35]. The mechanism most likely involves displacement of the labile PPh_3 ligand from [$RuCl_2(PPh_3)$(dppb)], which dimerizes to form the binuclear [RuCl(dppb)(μ-Cl)$_2$RuCl(dppb)] complex, followed by addition of amine to form the [RuCl(dppb)(μ-Cl)$_3$Ru(dppb)(amine)] complex.

Typical vibration bands in the FTIR spectrum confirmed the presence of Cl^- and amine in the isolated compound. The bands in the region of 345 and 310 cm^{-1} were attributed to ν(Ru–Cl) asymmetric and symmetric stretching vibrations, respectively, suggesting two *cis*-positioned Cl^- ligands (Fig. S1). In the ^{1}H NMR spectra, the peaks of the methylene hydrogen atoms (CH_2) of the coordinated amine and the carbon chain connecting the two phosphors in the dppb molecule showed signals between 0.0 and 3.1 ppm. Hydrogen bonded directly to the nitrogen atom in the amine showed a signal between 3.4 and 3.7 ppm. At low field, the spectra presented a set of signals relating to the aromatic rings of the dppb ligand between 6.7 and 8.3 ppm (Figs. S2–S4). In the $^{13}C\{^{1}H\}$ NMR spectra, the carbon peaks were observed between 22.0 and 140.4 ppm for the complexes **1**–**3**. The $^{31}P\{^{1}H\}$ NMR spectra showed a well-defined singlet at 49 ppm, confirming that the two phosphorus atoms are magnetically equivalent (Figs. S5–S7) [34]. For these configurations obtained for the complexes **1**–**3**, the appearance of two AB quartet patterns in the spectrum would be expected; however, the singlet observed in the $^{31}P\{^{1}H\}$ NMR spectra is presumably due to a rapid amine exchange process that renders the Ru centers and, consequently, results in the scrambling of all four phosphorus nuclei equivalent on the NMR time scale [35].

The electrochemical behavior of the complexes **1**–**3** was studied by cyclic voltammetry in the potential range of 0.0–1.8 V in CH_2Cl_2 solution containing 0.1 M of *n*-Bu_4NPF_6 as supporting electrolyte, with a scanning rate of 100 mV s^{-1}. The data of the cyclic voltammetry experiments are summarized in Table 1. The voltammograms of the complexes **1**–**3** are shown in Fig. 2. The complexes **1**–**2** underwent two successive single-electron oxidation processes, giving rise to the redox waves A and B in the potential region 0.30–1.40 V, referring to the Ru^{II}/Ru^{III} and Ru^{III}/Ru^{III} redox pairs. The presence of two redox pairs confirmed the formation of a dimeric species in which the {Ru(amine)(dppb)} fragment was connected via three μ-chloro bridges to a {RuCl(dppb)} moiety. As it can be observed from Fig. 1, the distinct fragments in the complexes **1**–**2** can be oxidized separately, showing two reversible one-electron oxidation steps. The electrochemical behavior of complex **3** showed only the redox pair of the fragment with $E_{1/2}$ of 0.41 V. However, the appearance of an anodic process around 1.0 V assigned to oxidation of the free amine (pep) in solution and the absence of the second Ru^{III}/Ru^{III} redox pair (process observed in the complexes **1** and **2**) lead us to rationalize that the process observed around 0.6 V could be associated with a ruthenium species without amine from the reversible dissociation of this ligand and that re-coordination to either Ru center occurs in these complexes. It is also important to consider that the pep ligand is the most hindered amine compared with the pop and pip ligands that would make the re-coordination of this ligand to the Ru center more difficult.

The electrochemical reversibility of the Ru^{II}/Ru^{III} redox pair of the complexes **1**–**3** was initially evaluated by calculating the potential difference (ΔE_p) of the values and comparing it with the ΔE_p of the ferrocene as a reference obtained under the same experimental conditions. According to the calculated values of the anode (E_{pa}) and cathode (E_{pc}) peaks, the complexes **1**–**3** show ΔE_p values lower than that of ferrocene, demonstrating redox reversibility (Table 1). Another criterion for reversibility is the anode/cathode peak current ratio equal to the unit and independent of the scan rate. This reversibility criterion was calculated for the complexes **1**–**3** at different potential scanning rates, and the I_{pa}/I_{pc} values were quite close to that expected for a reversible process ($I_{pa}/I_{pc} = 1$). The reversibility of the complexes was also evaluated by varying the scanning rates (Fig. 2-left). The cyclic voltammograms of the complexes **1**–**3** were typical voltammograms obtained for a reversible diffusion-controlled process. The graphs of I_{pc} and I_{pa} as a function of the square root of the scanning velocity are shown in Fig. 2-right. For a reversible process, the potential sweep velocity affects the I_p, and a linear relationship between I_p and $\nu^{1/2}$ is expected. Dependence of the current as a function of the square root

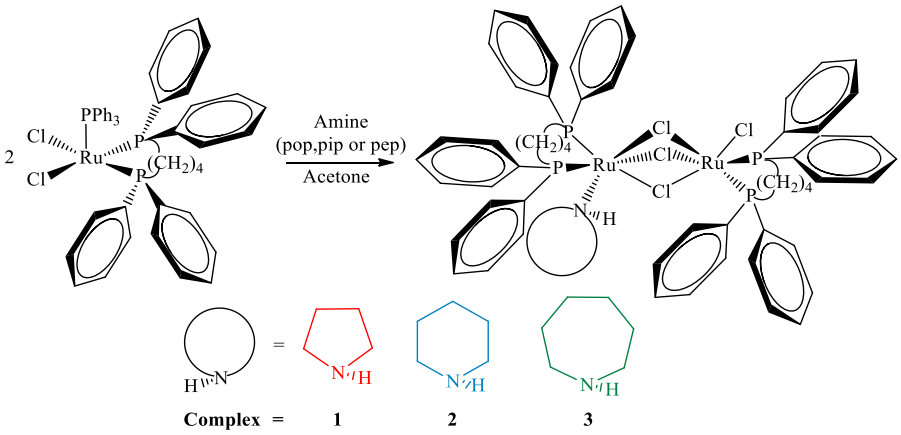

Scheme 1. Synthesis protocol of cyclic amine homobimetallic ruthenium complexes bearing a bidentate phosphine.

of the sweep speed was evaluated for the complexes **1**–**3**, and a linearity between I_p and $\nu^{1/2}$ was obtained.

The wave separation, or potential difference, $\Delta E_{1/2}$ and the comproportionation constant K_c are critical parameters for evaluating the thermodynamic stabilities of the oxidized states. As shown in Table 1, the $\Delta E_{1/2}$ and K_c values for the complexes **1** and **2** are around 0.84 and 0.87 V and 3.4×10^{14} and 7.5×10^{14}, respectively, which means that the $\Delta E_{1/2}$ and K_c values are undifferentiated (within experimental error), whereas for complex **3**, values of $\Delta E_{1/2} = 0.13$ V and $K_c = 506$ were observed. These results indicate that the first anodic potential (E_{paA}) has much more influence over the second anodic potential (E_{paB}) in complex **3** than in the other two complexes. This behavior was also observed in analogous binuclear ruthenium complexes containing dppb [36].

The absorption spectra of the complexes **1**–**3** (Fig. 3) showed a high absorption band with a maximum of 230 nm ($\varepsilon = 5.05 \times 10^4$ L mol^{-1} cm^{-1}) and one shoulder at 243 nm ($\varepsilon = 3.57 \times 10^4$ L mol^{-1} cm^{-1}) attributed to IL transfer of the amine and dppb. Other three bands are observed at 290 nm ($\varepsilon = 5.50 \times 10^3$ L mol^{-1} cm^{-1}), 380 nm ($\varepsilon = 2.0 \times 10^3$ L mol^{-1} cm^{-1}), and 486 nm ($\varepsilon = 0.32 \times 10^3$ L mol^{-1} cm^{-1}), and are probably associated with MLCT type transitions. The absorption spectra of the complexes **1**–**3** are very similar, suggesting that those complexes have the same geometric structure with the same qualitative configuration of the molecular orbital.

Table 1
Cyclic voltammetry[a] results for complexes **1**–**3**.

	CV		
	Complex 1	Complex 2	Complex 3
E_{paA} (mV)	470	470	460
E_{pcA} (mV)	350	350	350
E_{paB} (mV)	1310	1340	590
E_{pcB} (mV)	1240	1250	530
$E_{1/2A}$ (mV)	410	410	400
$E_{1/2B}$ (mV)	1270	1290	560
ΔE_{pA} (mV)	120	120	110
ΔE_{pB} (mV)	70	90	60
I_{paA}/I_{pcA} (mA)	1.01	0.96	0.97
$\Delta E_{1/2}$ (mV)[b]	860	880	160
K_c[c]	3.45×10^{14}	7.52×10^{14}	506.79

[a] Conditions: CH_2Cl_2, n-Bu_4NPF_6 (supporting electrolyte, 0.1 mol L^{-1}), [Ru] = 10 mmol L^{-1}, scan rate = 100 mV s^{-1}), platinum disk and wire (working and auxiliary electrode), Ag/AgCl (reference electrode). $E_{1/2}$ is the half-potential for the complex; ΔE_p is the cathodic-anodic peak separation. The potential difference (ΔE_p) and I_{pa}/I_{pc} values of the [Fc]/[Fc]$^+$ couple under these conditions are 0.24 V and 1.09, respectively.

[b] $\Delta E_{1/2} = E_{1/2B} - E_{1/2A}$ denotes the potential difference between redox processes A and B.

[c] The comproportionation constants, K_c, were calculated by the formula $K_c = \exp(\Delta E_{1/2}/25.69)$ at 298 K [36].

3.2. ROMP reactions

In order to assess the catalytic efficiency of the amine-ruthenium(II) complexes **1**–**3**, ring-opening metathesis polymerization (ROMP) of norbornene (NBE) was attempted in $CHCl_3$ at 25 and 50 °C with a [NBE]/[Ru] ratio of 5000. Under these conditions, the complexes **1**–**3** were completely inefficient. In contrast, when ethyl diazoacetate (EDA) was added to generate metathetically active ruthenium–carbene species from the [RuCl(dppb)(μ-Cl)$_3$Ru(dppb)(amine)] precursors **1**–**3**, ROMP occurred with moderate yields (Scheme 2).

In previous studies conducted by our research group, variation in EDA concentration in NBE ROMP using ruthenium complexes directly influenced the catalytic activity of the catalysts [19,37–39]. In these studies, a continuous increase in polyNBE yields and M_n values was observed when the molar ratio was used up to [EDA]/[Ru] = 28. For [EDA]/[Ru] > 28 ratios, the yield values showed a marked decrease, where an excessive amount of EDA probably competes with the monomer in coordination with the metal. Thus, the [EDA]/[Ru] = 28 ratio was adopted in all ROMP experiments in the present study.

Fig. 4 shows an increase in the yields when increasing reaction time for all complexes at 25 °C. The following order of reactivity was observed when the activity of the complexes **1**–**3** was compared: **3** > **2** > **1**. This order of activity could be associated with the higher Ru → olefin synergism, given the σ-donor characteristic of the pep, pip and pop ligands. The observed profile is within the expected range because as the larger the number of CH_2 groups in the ring of the cyclic amine, the greater the donor power of the amine, which favors the synergism amine → Ru → olefin. Improvement of activity is achieved with the contribution of two factors: metal carbene species formation and olefin activation; both criteria seam to be favored from **1** to **3** as the yields increase from 54% to 62%, respectively. Comparison between the three complexes showed that complex **3** was much more active than its two similar complexes at earlier times. The more pronounced increase in yield at the beginning of polymerization could be associated with the increase in steric hindrance exerted by the pep ligand, which favors the release of ligands from the Ru center during the induction period.

Fig. 5 shows the profile of the molecular weights and PDIs as a function of time, in which a slight increase in the M_n values could

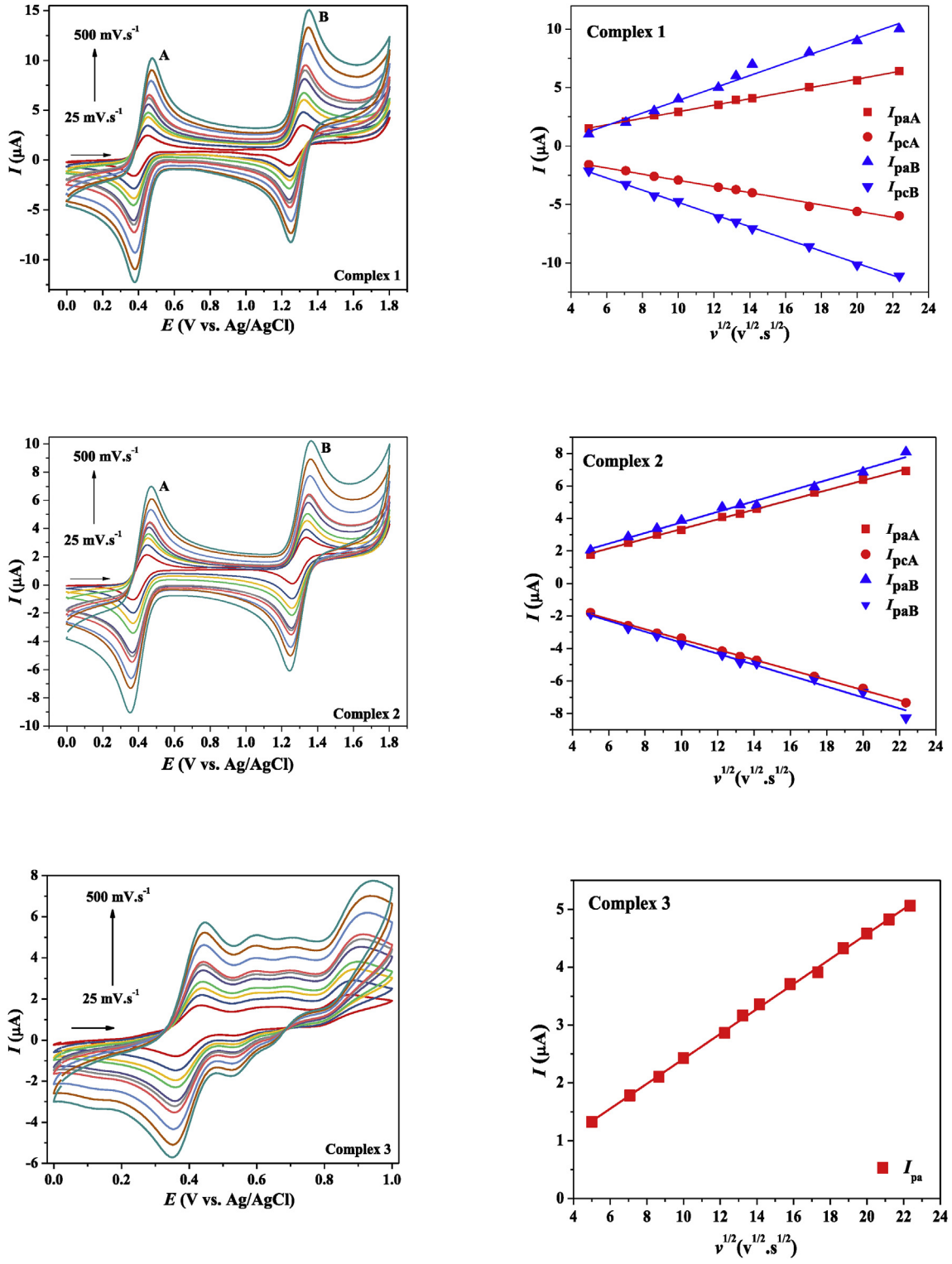

Fig. 2. Left - Cyclic voltammograms of the complexes **1**–**3** in CH_2Cl_2 at 25 °C. [Ru] = 10 mmol L^{-1}; [*n*-Bu_4NPF_6] = 0.1 mol L^{-1}; scanning anodically from 0.0 up to 1.8 V for complexes **1**–**2** and up to 1.0.V for complex **3** at scan rates of 25, 50, 75, 100, 150, 175, 200, 300, 400 and 500 mV s^{-1}. Rigth - Current (*I*) of the anodic (I_{pa}) and cathodic (I_{pc}) processes vs. square root of the potential scan rate (ν).

be observed in the beginning of polymerization (Fig. S8), followed by an abrupt increase after 30 min with moderate PDIs. In general, polymers synthesized using complex **3** showed higher M_n values and narrower molecular weight distribution than those synthesized using complex **2** and these, in turn, were smaller than those using complex **1**. It is believed that the increased steric hindrance caused by the cyclic amine in the following order: pop < pip < pep, provides a faster leaving of dppb ligand for metal carbene species formation or coordination of the olefin. In the ROMP experiments in the presence of 20-fold excess of dppb, the yields of polyNBE were

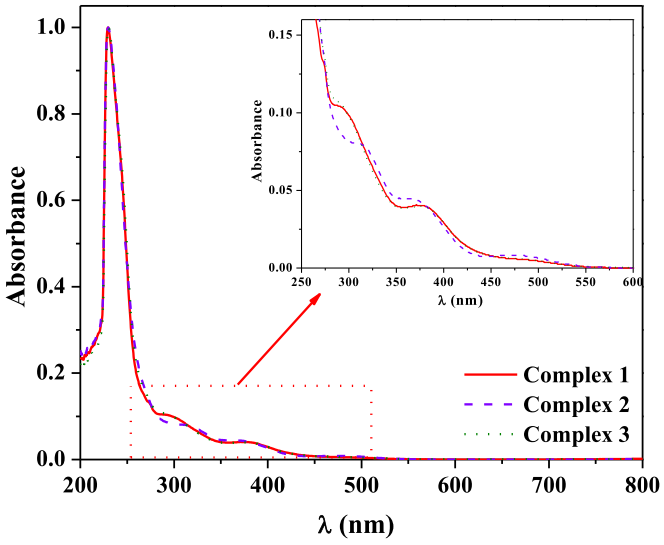

Fig. 3. Electronic spectra of the complexes **1**–**3** in degassed CH_2Cl_2 solution at 25 °C ([Ru] = 0.1 mmol L^{-1}).

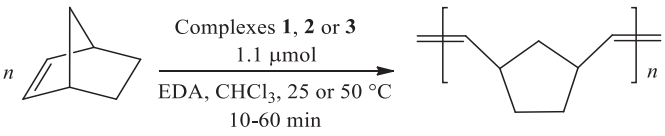

Scheme 2. ROMP of NBE catalyzed by complexes **1**–**3**.

less than 1% of polyNBE, whereas the yields of polyNBE in the presence of amine (20 ×) were practically unchanged when using [NBE]/[EDA]/[Ru] = 5000/28/1 for 60 min at 25 °C. Probably, the presence of dppb in solution suppresses the living of dppb ligand, thus preventing the ROMP reaction. These experiments support that the ROMP reaction using the complexes **1**–**3** depends on the lability of the dppb ligands, considering that polymerization was inhibited in the presence of dppb. Further, free dppb was observed in $^{31}P\{^1H\}$ NMR studies simulating the induction period of ROMP with the complexes **1**–**3** ([EDA]/[Ru] = 28), supporting the leaving

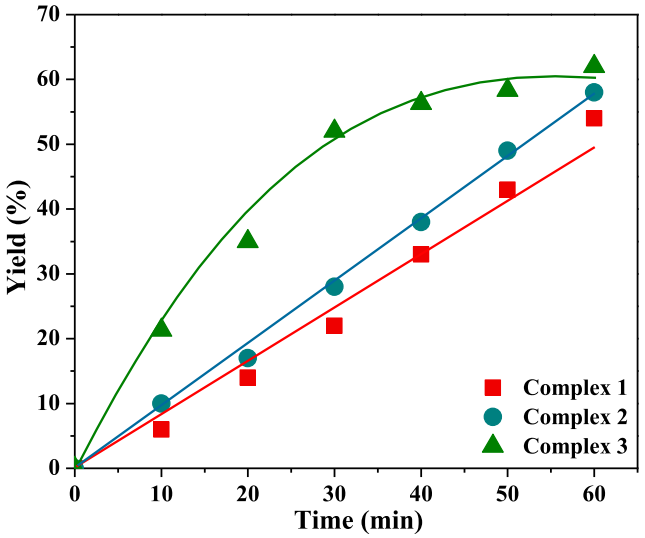

Fig. 4. Dependence of yield as a function of time for ROMP of NBE with **1** (■), **2** (●) and **3** (▲); [NBE]/[Ru] = 5000 and [EDA]/[Ru] = 28 ratios in $CHCl_3$ at 25 °C.

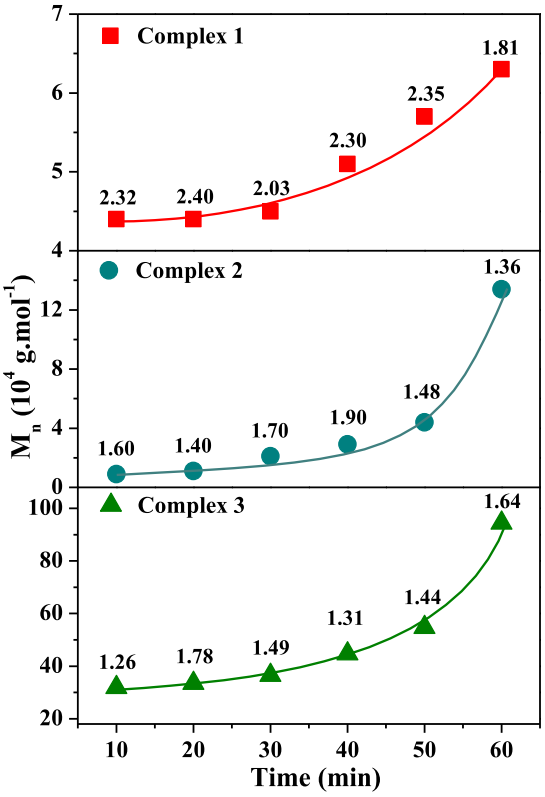

Fig. 5. SEC data from the ROMP of NBE with the complexes **1**–**3** at 25 °C; [NBE]/[Ru] = 5000 and [EDA]/[Ru] = 28 ratios with 1.1 μmol of complex in $CHCl_3$.

of dppb for the formation of metal-carbene species.

ROMP of NBE was also evaluated at 50 °C for the complexes **1**–**3** under the same conditions. It was observed that the yields of polyNBE increased with increasing temperature (Fig. 6), reaching an order of magnitude of 10^5 g mol^{-1} (Figs. 7 and S9). For complex **3**, decreased yields and molecular weights were observed after 40 min, which is an indication of secondary reactions. The increase in yield and molecular weight values as compared at 25 °C could be associated with favoring the leaving of ligands for the coordination of NBE. The order of catalytic activity of the complexes in ROMP was maintained: **3** > **2** > **1**, with complex **3** reaching quantitative yield in 40 min.

Catalytic activities of **1**–**3** for ROMP of NBD were also tested at 25 and 50 °C with a [NBD]/[Ru] ratio of 5000 for 60 min. The complexes showed low catalytic activity (6–11%) at 25 °C. Besides the catalytic tests performed at 25 °C, the polymerizations were also conducted at 50 °C under the same conditions. The increase of temperature produced higher yields of polyNBD (14–45%) in relation to 25 °C in all cases. The polyNBD were insoluble in THF.

3.3. ATRP reactions

Attention is now focused on the atom-transfer radical polymerization (ATRP) of methyl methacrylate (MMA) initiated by ethyl-2-bromoisobutyrate (Scheme 3). The complexes **1**–**3** present properties that make them promising compounds for use as ATRP catalysts. They provide reversible Ru^{II}/Ru^{III} pairs at easily accessible potentials, as shown by the electrochemical data. Polymerization of MMA via ATRP with the complexes **1**–**3** was performed as a function of time using a [MMA]/[EB*i*B]/[Ru] ratio of 1000/2/1 M ratio at 85 °C, and it was shown that all catalysts could mediate radical polymerizations of MMA. The MMA conversion values increase

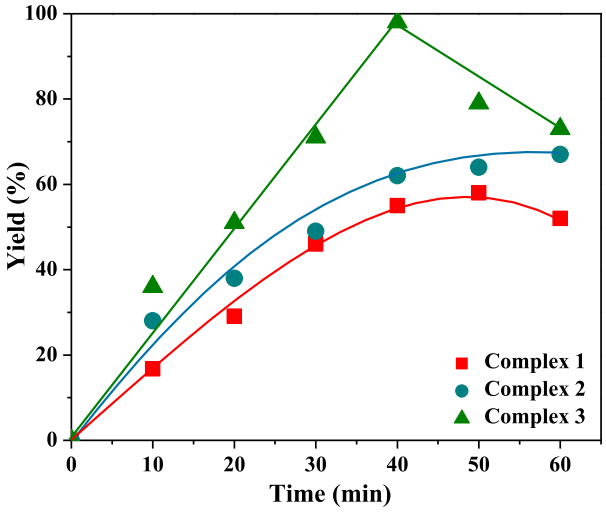

Fig. 6. Dependence of yield as a function of time for ROMP of NBE with **1** (■), **2** (●), and **3** (▲); [NBE]/[Ru] = 5000 and [EDA]/[Ru] = 28 ratios in $CHCl_3$ at 50 °C.

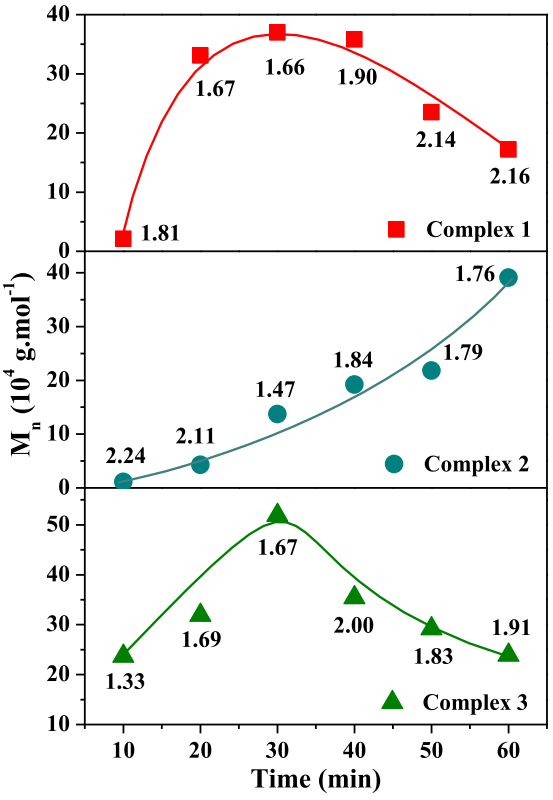

Fig. 7. SEC data from the ROMP of NBE with the complexes **1**–**3** at 25 °C; [NBE]/[Ru] = 5000 and [EDA]/[Ru] = 28 ratios with 1.1 μmol of complex in $CHCl_3$.

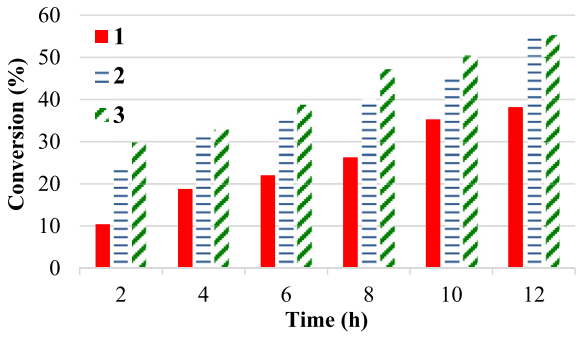

Fig. 8. Dependence of conversion on the reaction time for ATRP of MMA with **1**–**3**; [MMA]/[EBiB]/[Ru] = 1000/2/1 ratio with 12 μmol of complex in toluene at 85 °C.

linearly as a function of time in all cases (Fig. 8). The catalytic activity of the complexes **1**–**3** has increased with the increase of the CH_2 groups on the ring of the cyclic amine. The complex **1** achieved a maximum conversion of 38% of polyMMA, while the complex **3** reached 55% in 12 h.

As observed in the ROMP, the order of reactivity observed is **3** > **2** > **1**. This trend could be explained by the increase of the steric hindrance of the amine, which promotes a greater lability of the metal-halide bond in the dormant species, favoring the production of propagating radicals. This difference in activity is exclusively related to steric factors, once there are no differences in the oxidation potentials of the complexes **1**–**3** (Table 1).

The plot of $\ln([MMA]_0/[MMA]_t)$ as a function of reaction time shows an asymptotic relationship for all catalysts, revealing that the radical concentration is not constant during MMA polymerization. In contrast, Fig. 9 shows that the polyMMA molecular weights of the order of 10^4 g mol^{-1} obtained with the complexes **1**–**3** increased as a function of MMA conversion. Evolution of the molecular weights with conversion together with an example of GPC traces are also shown in Fig. 9 and S10. Although the GPC curves of the polyMMAs showed a monomodal distribution and shifted to higher values with conversion (Fig. 9), the molecular weights were much higher than those theoretically predicted in all cases (Table 2). The molecular weight that came closer to the theoretical ones was obtained with complex **3**. These results corroborate the polydispersity values (PDI) of the polymers, above each point in Fig. 9, because the narrower molecular weight distributions were obtained with complex **3**, which indicates that a certain level of control was achieved with mediation by this complex. Although the controlling ability was poor ($M_{n(exp)} \gg M_{n(theor)}$, high polydispersity), the sustained polymerization and the M_n growth with conversion demonstrated the reversibility of atom transfer in the ATRP equilibrium.

4. Conclusions

The novel complexes [RuCl(dppb)(μ-Cl)$_3$Ru(dppb)(pop)] (**1**), [RuCl(dppb)(μ-Cl)$_3$Ru(dppb)(pip)] (**2**), and [RuCl(dppb)(μ-

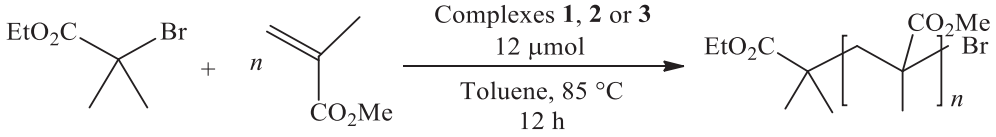

Scheme 3. ATRP of MMA catalyzed by Ru-amine complexes.

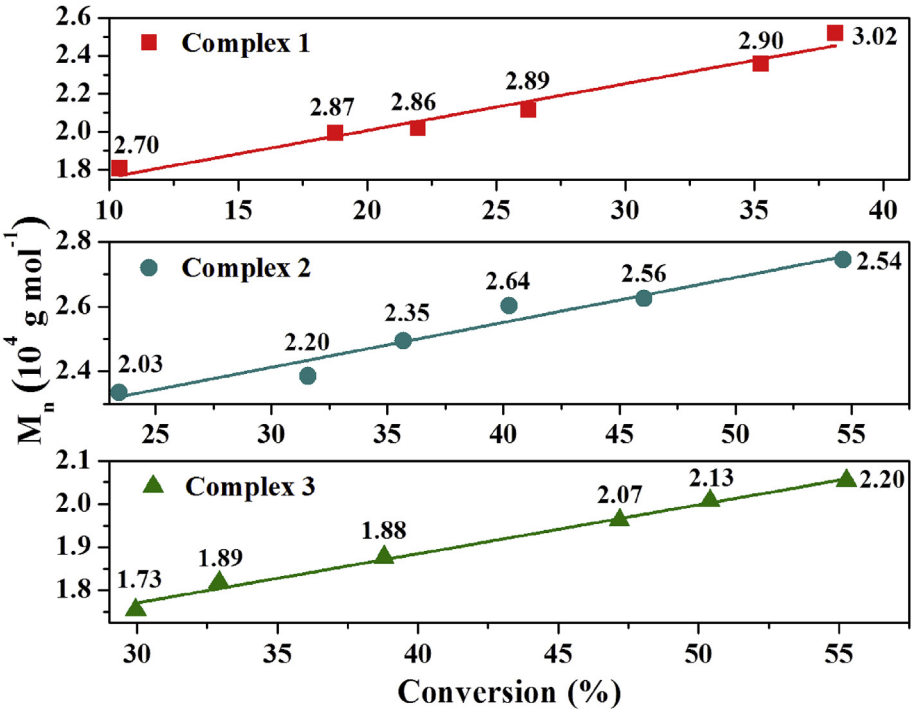

Fig. 9. SEC data from the ATRP of MMA with the complexes **1**–**3** at 85 °C; [MMA]/[EBiB]/[Ru] = 1000/2/1 ratio with 12 μmol of complex in toluene.

$Cl)_3$Ru(dppb)(pep)] (**3**) were successfully synthesized and characterized by elemental analysis, FTIR, UV–Vis, and ^{1}H, ^{13}C{^{1}H} and ^{31}P{^{1}H} NMR spectroscopy. The electrochemistry properties of the complexes **1**–**3** were investigated by cyclic voltammetry and exhibited two successive single-electron oxidation processes. The presence of two redox pairs confirms the formation of a dimeric species in which the {Ru(amine)(dppb)} fragment was connected via three μ-chloro bridges to a {RuCl(dppb)} moiety. Complexes **1**–**3** showed good catalytic activity in the NBE ROMP polymerization reaction in the presence of 5 μL EDA with [NBE]/[Ru] = 5000 M ratio at 25 and 50 °C. A significant increase in yield values was observed with increasing temperature from 25 to 50 °C in all cases. This behavior may be associated with favoring the lability of a ligand to the substrate entrapment. The catalytic activity of the complexes **1**–**3** showed the following order of reactivity: **3** > **2** > **1**. This order of catalytic activity may be associated with the greater amine → Ru → olefin synergism, given the strong σ-donor characteristic of the pep, pip and pop amines. MMA polymerization mediated by the complexes **1**–**3** via ATRP was performed using a [MMA]/[EBiB]/[Ru] = 1000/2/1 M ratio at 85 °C. The molecular weight of polyMMA obtained with the complexes **1**–**3** increase linearly as a function of MMA conversion. However, the molecular weights were much higher than those theoretically predicted in all cases. The molecular weight that came closer to the theoretical

Table 2
ATRP[a] of MMA using complexes **1**, **2** or **3**.

	Time (h)	Conversion[b] (%)	$M_{n,exp}$[c] (10^4 g mol^{-1})	$M_{n,theor}$[d] (10^4 g mol^{-1})	PDI[c]
Complex **1**	2	10.41	1.81	0.52	2.70
	4	18.77	1.99	0.94	2.87
	6	21.98	2.02	1.10	2.86
	8	26.25	2.11	1.31	2.89
	10	35.27	2.35	1.77	2.90
	12	38.15	2.52	1.91	3.02
Complex **2**	2	23.42	2.33	1.17	2.03
	4	31.56	2.39	1.58	2.20
	6	35.69	2.49	1.79	2.35
	8	40.23	2.60	2.01	2.64
	10	46.06	2.63	2.31	2.56
	12	54.63	2.75	2.73	2.54
Complex **3**	2	29.95	1.75	1.50	1.73
	4	32.91	1.82	1.65	1.89
	6	38.79	1.88	1.94	1.88
	8	47.17	1.96	2.36	2.07
	10	50.39	2.01	2.52	2.13
	12	55.26	2.05	2.77	2.20

[a] [MMA]/[EBiB]/[Ru] = 1000/2/1 at 85 °C.
[b] Determined by GC.
[c] Determined by GPC in THF.
[d] $M_{n,theor}$ = [MMA]/[EBiB] × $M_{w,MMA}$ × conversion.

ones was obtained with complex **3**, indicating that a certain level of control was achieved in MMA polymerization with mediation by this complex.

Acknowledgements

The authors are indebted to the financial support from FAPESP (V. P. Carvalho-Jr: Proc. 2018/06340-1 and B. S. Lima-Neto: Proc. 2017/06329-5). This study was financed in part by Coordenação de Aperfeiçoamento de Pessoal de Nível Superior − Brasil (CAPES) − Finance Code 001.

Appendix A. Supplementary data

Supplementary data to this article can be found online at https://doi.org/10.1016/j.molstruc.2019.126874.

References

[1] R. Poli, Angew. Chem. Int. Ed. 45 (2006) 5058.
[2] R. Poli, Eur. J. Inorg. Chem. (2011) 1513.
[3] M. Kamigaito, T. Ando, M. Sawamoto, Chem. Rev. 101 (2001) 3689.
[4] K. Matyjaszewski, J.H. Xia, Chem. Rev. 101 (2001) 2921.
[5] F. di Lena, K. Matyjaszewski, Prog. Polym. Sci. 35 (2010) 959.
[6] N.V. Tsarevsky, K. Matyjaszewski, Chem. Rev. 107 (2007) 2270.
[7] K. Matyjaszewski, Macromolecules 45 (2012) 4015.
[8] K. Matyjaszewski, N.V. Tsarevsky, Nat. Chem. 1 (2009) 276.
[9] W. Tang, K. Matyjaszewski, Macromolecules 39 (2006) 4953.
[10] W. Tang, Y. Kwak, W. Braunecker, N.V. Tsarevsky, M.L. Coote, K. Matyjaszewski, J. Am. Chem. Soc. 130 (2008) 10702.
[11] T. Ando, M. Kamigaito, M. Sawamoto, Tetrahedron 53 (1997) 15445.
[12] J. Ueda, M. Matsuyama, M. Kamigaito, M. Sawamoto, Macromolecules 31 (1998) 557.
[13] P.W. Armit, A.S.F. Boyd, T.A. Stephenson, J. Chem. Soc. Dalton Trans. (1975) 1663.
[14] P.R. Hoffman, K.G. Caulton, J. Am. Chem. Soc. 97 (1975) 4221.
[15] R.C.J. Vriends, G. van Koten, K. Vrieze, Inorg. Chim. Acta 26 (1978) L29.
[16] J.M.E. Matos, B.S. Lima-Neto, J. Mol. Catal. A Chem. 222 (2004) 81.
[17] J.M.E. Matos, B.S. Lima-Neto, J. Mol. Catal. A Chem. 259 (2006) 286.
[18] J.L. Silva Sá, B.S. Lima-Neto, J. Mol. Catal. A Chem. 304 (2009) 187.
[19] V.P. Carvalho, C.P. Ferraz, B.S. Lima-Neto, J. Mol. Catal. A Chem. 333 (2010) 46.
[20] J.L. Silva Sá, L.H. Vieira, E.S.P. Nascimento, B.S. Lima-Neto, Appl. Catal. 374 (2010) 194.
[21] L.R. Fonseca, J.L. Silva Sá, E.S.P. Nascimento, B.S. Lima-Neto, New J. Chem. 39 (2015) 4063.
[22] R.A.N. Silva, P. Borim, L.R. Fonseca, B.S. Lima-Neto, J.L.S. Sá, V.P. Carvalho Jr., Catal. Lett. 147 (2017) 1144.
[23] V. Dragutan, I. Dragutan, J. Organomet. Chem. 691 (2006) 5129.
[24] T. Ando, M. Kamigaito, M. Sawamoto, Macromelecules 33 (2000) 6732.
[25] C.W. Jung, P.E. Garrou, P.R. Hoffman, K.G. Caulton, Inorg. Chem. 23 (1984) 726.
[26] F. Simal, D. Jan, L. Delaude, A. Demonceau, M.R. Spirlet, A.F. Noels, Can. J. Chem. 79 (2001) 529.
[27] F. Simal, A. Demonceau, A.F. Noels, Angew. Chem. Int. Ed. 38 (1999) 538.
[28] T. Opstal, F. Verpoort, Polym. Bull. 50 (2003) 17.
[29] A.M. Villa-Hernández, C.P. Rosales-Velázquez, E. Saldívar-Guerrab, J.R. Torres-Lubián, J. Braz. Chem. Soc. 22 (2011) 2070.
[30] M. Kamigaito, Y. Watanabe, T. Ando, M. Sawamoto, J. Am. Chem. Soc. 124 (2002) 9994.
[31] C. Aguilar-lugo, R. LeLagadec, A.D. Ryabov, G.C. Valverde, S.L. Morales, L. Alexandrova, J. Polym. Sci. Part A Polym. Chem. 47 (2009) 3814.
[32] T. Opstal, F. Verpoort, New J. Chem. 27 (2003) 257.
[33] X. Sauvage, Y. Borguet, A.F. Noels, L. Delaude, A. Demonceau, Adv. Synth. Catal. 349 (2007) 255.
[34] A.M. Joshi, I.S. Thorburn, S.J. Rettig, B.R. James, Inorg. Chim. Acta 198−200 (1992) 283.
[35] D.E. Fogg, B.R. James, Inorg. Chem. 34 (1995) 2557.
[36] D.E. Richardson, H. Taube, Inorg. Chem. 20 (1981) 1278.
[37] P. Borim, B.S. Lima-Neto, B.E. Goi, V.P. Carvalho Jr., Inorg. Chim. Acta 456 (2017) 171.
[38] M.B.A. Afonso, Y.F. Silva, J.C.A. Pereira, A.E.H. Machado, B.E. Goi, B.S. Lima-Neto, V.P. Carvalho Jr., J. Organomet. Chem. 851 (2017) 225.
[39] T.R. Cruz, R.A.N. Silva, A. Machado, B.S. Lima-Neto, B.E. Goi, V.P. Carvalho Jr., New J. Chem. 43 (2019) 6220.